

# Quantum memory assisted observable estimation

Liubov Markovich,<sup>1,2,3,\*</sup> Attaallah Almasi,<sup>1,†</sup> Sina Zeytinoglu,<sup>4,5,‡</sup> and Johannes Borregaard<sup>1,§</sup>

<sup>1</sup>*QuTech and Kavli Institute of Nanoscience, Delft University of Technology, 2628 CJ, Delft, The Netherlands*

<sup>2</sup>*Instituut-Lorentz, Universiteit Leiden, P.O. Box 9506, 2300 RA Leiden, The Netherlands*

<sup>3</sup>*Institute for information transmission problems, Bol. Karetny per. 19, Moscow 127051, Russia*

<sup>4</sup>*Department of Physics, Harvard University, Cambridge, Massachusetts 02138, USA*

<sup>5</sup>*Physics and Informatics Laboratory, NTT Research, Inc., Sunnyvale, California, 94085, USA*

(Dated: December 16, 2022)

The estimation of many-qubit observables is an essential task of quantum information processing. The generally applicable approach is to decompose the observables into weighted sums of multi-qubit Pauli strings, i.e., tensor products of single-qubit Pauli matrices, which can readily be measured with single qubit rotations. The accumulation of shot noise in this approach, however, severely limits the achievable precision for a finite number of measurements. We introduce a novel method, called Coherent Pauli Summation (CPS) that circumvents this limitation by exploiting access to a single-qubit quantum memory in which measurement information can be stored and accumulated. Our algorithm offers a reduction in the required number of measurements, for a given precision that scales linearly with the number of Pauli strings of the decomposed observable. Our work demonstrates how a single long-coherence qubit memory can assist the operation of noisy many-qubit quantum devices in a cardinal task.

Noisy intermediate scale quantum (NISQ) devices with up to hundreds of qubits have been realized with superconducting hardware [1, 2], neutral atoms [3, 4], and trapped ions [5–7]. These advancements stimulated interest for simulating many-body systems such as the electronic structure of molecules [8], studying non-equilibrium quantum statistical mechanics [9], and performing combinatorial optimization [10] on such devices. A cardinal task for many of these applications is to estimate expectation values of many-qubit observables such as the energy of the system. The direct estimation of such observables can be highly non-trivial for, e.g., fermionic observables simulated on qubit systems [11] and poses a significant challenge for NISQ devices due to large measurement circuit depths and overall sampling complexity i.e. total number of measurements for a required estimation precision.

One approach for observable estimation with minimal sampling complexity is the quantum phase estimation (QPE) algorithm [12–17]. Its implementation, however, requires qubit systems with low noise and long coherence times for high precision estimation since the measurement circuit depth is inversely proportional to the achievable precision. This renders it outside the scope of NISQ devices.

As an alternative, the quantum energy (expectation) estimation (QEE) approach of decomposing the observable into a weighted sum of  $N$  multi-qubit Pauli strings is commonly used in the variational quantum eigensolver [18]. While QEE minimizes the measurement circuit depth by requiring only a single layer of single-qubit rotations, it also suffers from increased sample complexity due to the accumulation of shot noise in the estimation procedure. Specifically, Pauli strings are estimated independently and the observable is then calculated as a linear combination of these.

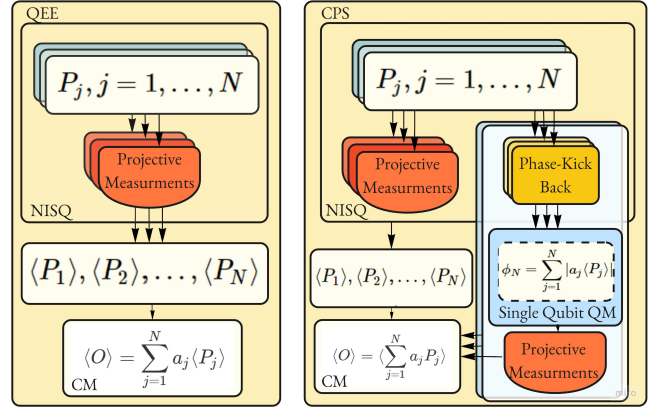


FIG. 1. The comparison of QEE and our CPS method. On the left, the QEE method, where the expectation value of each Pauli string is estimated by a series of projective measurements and the summation of all  $\langle P_j \rangle$ ,  $j = 1, \dots, N$  is done classically to obtain an estimate of the observable  $\langle O \rangle$ . On the right, the CPS method, where  $\langle P_j \rangle$  is encoded in the single qubit quantum memory such that a direct encoding of  $\langle O \rangle$  is obtained. In addition, a small amount of projective measurements of each Pauli string is also being performed for correction purposes. After the encoding process is done, a final projective measurement on the quantum memory qubit is performed. The procedure is then iterated to obtain an estimate of  $\langle O \rangle$  to the desired precision.

Consequently, to estimate an observable comprised of  $N$  Pauli strings to a precision  $\eta$ , each Pauli string should be estimated to a precision  $O(\eta/N)$  resulting in an overall sample complexity scaling as  $O(N^2)$ . This accumulation of noise poses a “shot noise bottleneck” since the amount of measurements will ultimately be limited by the available run time of the device before e.g. re-calibration of

the device is needed. The measurement process itself is also often one of the most time consuming operations in current quantum devices [1, 5, 6].

To tackle the shot noise bottleneck, recent works have considered intermediate approaches between QPE and QEE to obtain better precision in the estimation of the individual Pauli strings [19] or methods for grouping Pauli strings in commuting sets to reduce the sample complexity [20, 21]. While both approaches have the potential to reduce the overall sample complexity neither improves the fundamental scaling of the noise accumulation with the number of Pauli strings in the observable decomposition.

In this article, we describe a novel algorithm called the Coherent Pauli Summation (CPS) method that overcomes the shot-noise bottleneck through the use of a single-qubit quantum memory (QM). Our method allows for a direct measurement of the multi-qubit observable by estimating the phase of the memory qubit at the end of the protocol. Hence, the accumulation of shot noise, originating from the summation of individually estimated mean values of Pauli strings in the QEE approach, is prevented. Importantly, this is obtained with a measurement circuit depth that scales only logarithmic with the required estimation precision in contrast to the linear scaling of the QPE algorithm.

The critical point of the CPS method is to employ Quantum Signal Processing (QSP) techniques to encode the mean value of Pauli strings in the phase of a single qubit quantum memory. The lack of shot noise accumulation results in a gain in the variance of the estimate compared to the QEE method of  $O(1/N)$ , where  $N$  is the number of Pauli strings in the observable decomposition. This gain can be understood as obtaining a Heisenberg limited scaling of the variance rather than the standard quantum limit scaling of the QEE method. The necessary coherence time of the single memory qubit required for CPS scales linearly with  $N$  while the required coherence time overhead of the NISQ device only increases logarithmic with the required precision. The CPS method thus outlines how a single long-coherence qubit memory can advance the performance of larger scale NISQ devices.

In order to set the stage of our algorithm, we first review the basic steps of the standard QEE approach. The first step of the QEE approach for estimating the expectation value of an observable  $O$  for a given quantum state  $|\Psi\rangle$ , is to decompose it into a weighted sum of Pauli strings

$$O = \sum_{j=1}^N a_j P_j, \quad (1)$$

where  $a_j$  are the (real) decomposition coefficients and  $P_j$  are the Pauli strings composed as tensor products of single qubit Pauli matrices and the identity. This decomposition is always possible since a collection of  $d^2$  Pauli

strings forms a complete operator basis for a  $d$  dimensional Hilbert space. Note, however, that the number of Pauli strings,  $N$ , in the decomposition can be very large for a general multi-qubit observable. For example, when mapping fermionic systems on to qubit quantum devices, local fermionic observables can map to multi-qubit observables spanning the device [22–24].

In the QEE approach, the state  $|\Psi\rangle$  is repeatedly prepared and the Pauli strings are measured sequentially via single qubit projective measurements to obtain estimates of every Pauli string:  $\langle P_j \rangle \equiv \langle \Psi | P_j | \Psi \rangle$  [18, 25]. The mean value of the observable  $\langle O \rangle$  can be calculated classically after estimating all  $\langle P_j \rangle$ ,  $j = 1, \bar{N}$ . This approach, however, suffers from the accumulation of shot noise from the individually estimated mean values of the Pauli strings as described above. If each estimate  $\langle \hat{P}_j \rangle$  is estimated with a variance  $\sigma^2(\langle \hat{P}_j \rangle) \sim \eta_p$ , the variance of the final estimate is  $\sigma^2(\langle \hat{O} \rangle) \sim N \eta_p$  assuming roughly equal weights of the  $P_j$  in the decomposition of  $O$ .

We now outline our proposed CPS method that circumvents this accumulation of shot noise. A high-level outline of the protocol is shown in Fig. 1. Let  $|\Psi_0\rangle \equiv V|0\rangle$  be a quantum state of the NISQ device, where  $V$  is an invertible preparation circuit. The state  $|0\rangle$  denotes the state where all qubits are prepared in their ground state  $|0\rangle$ . Let  $\langle \Psi_0 | O | \Psi_0 \rangle$  be the expectation value we want to estimate within a variance of  $\eta$ . The three steps of the CPS method are:

1. Obtain rough estimates of the mean values of every Pauli string  $\langle \Psi_0 | P_j | \Psi_0 \rangle$ ,  $j = 1, \dots, N$  by performing  $O\left(\log\left(\frac{N}{\sqrt{\eta}}\right)\right)$  projective measurements similar to the QEE approach. This step estimates  $\tau_j = \text{sign}(a_j \langle P_j \rangle)$  i.e. the sign information of the Pauli strings.
2. In the second step,  $\tilde{\epsilon}_0 \tau_j |a_j \langle \Psi_0 | P_j | \Psi_0 \rangle|$  is directly encoded in the phase of the single qubit memory using a modified phase-kick back algorithm [26] together with QSP techniques. This is done sequentially for all Pauli strings in the decomposition resulting in a final phase of  $\sim \tilde{\epsilon}_0 \langle \Psi_0 | O | \Psi_0 \rangle$  followed by a projective measurement of the single qubit state.
3. The previous step is repeated  $M_0$  times to obtain an estimate of  $2^0 \tilde{\epsilon}_0 \langle \Psi_0 | O | \Psi_0 \rangle$  and the whole procedure is repeated  $M_l = \alpha + \gamma(d_L + 1 - l)$  times for every  $2^l \tilde{\epsilon}_0$ ,  $l = 1, 2, \dots, d_L$ ,  $d_L = \lceil \log_2 1/\eta \rceil$ ,  $\alpha > 2$  and  $\gamma > 0$ . The increasing powers of  $\tilde{\epsilon}_0$  enables estimation of the digits of  $\langle \Psi_0 | O | \Psi_0 \rangle$ , thereby circumventing the  $2\pi$  ambiguity of the phase estimation. The total amount of repetitions of the second step with different powers of  $\tilde{\epsilon}_0$  is  $M_q = 2 \sum_{l=0}^{d_L} M_l$ .

At the end of these three steps,  $\langle \Psi_0 | O | \Psi_0 \rangle$  is estimated to precision  $\eta$  with an overall sample complexity

of  $NO\left(\frac{\log(N/\sqrt{\eta})}{\log\log(N/\sqrt{\eta})}\right)$ . We have counted this scaling as the number of state preparation circuits  $V$  required in the method which also includes the extra state preparation circuits that are part of the QSP step as detailed below.

The second step as defined above is the main step of the CPS method. We will now go through this in details. The first operation in this step is to prepare the state

$$|\tilde{\Psi}_0\rangle_j \equiv \sqrt{1-\epsilon_j}|0\rangle_p|\Psi_0\rangle + \sqrt{\epsilon_j}|1\rangle_p|\Psi_j\rangle, \quad (2)$$

by applying a controlled Pauli operator,  $CP_j = |0\rangle_p\langle 0| \otimes I + |1\rangle_p\langle 1| \otimes P_j$ , between an auxiliary qubit (control) prepared in state  $|a\rangle_p = (\sqrt{1-\epsilon_j}|0\rangle_p + \sqrt{\epsilon_j}|1\rangle_p)$  and the multi-qubit state  $|\Psi_0\rangle$  (target). Here  $I$  is identity,  $P_j$  is the  $j$ 'th Pauli string in the decomposition of  $O$ , and we have defined  $|\Psi_j\rangle \equiv P_j|\Psi_0\rangle$ . The parameter  $\epsilon_j$  relates to the decomposition coefficients of  $O$  (see Eqn. (1)) as  $\sqrt{\epsilon_j(1-\epsilon_j)} = |a_j|\sqrt{\epsilon}$ , where  $\epsilon_j, \epsilon \in (0, 1)$ . To ease notation, we will denote the entire preparation circuit of  $|\tilde{\Psi}_0\rangle_j$  as  $\tilde{V}_j$  i.e.  $\tilde{V}_j|0\rangle = |\tilde{\Psi}_0\rangle_j$ .

We now introduce the state  $|\tilde{\Psi}_1\rangle_j \equiv (\sigma_x \otimes I)|\tilde{\Psi}_0\rangle_j$  from which it follows that  $|\langle\tilde{\Psi}_0|\tilde{\Psi}_1\rangle_j| = \tilde{\epsilon}_0|a_j\langle\Psi_0|P_j|\Psi_0\rangle| = \tilde{\epsilon}_0|a_j\langle P_j\rangle|$ , where  $\tilde{\epsilon}_0 \equiv 2\sqrt{\epsilon}$ , holds. Similar to the phase kickback method in Ref. [26], we consider the operator  $U_{P_j} = \tilde{V}_j\Pi_0\tilde{V}_j^\dagger P_j$ , where  $\Pi_0 = I - 2|0\rangle\langle 0|$ . The action of  $U_{P_j}$  is a rotation by a principal angle  $\theta_j = \arccos(\tilde{\epsilon}_0|a_j\langle P_j\rangle|)$  in the subspace spanned by  $|\tilde{\Psi}_0\rangle_j$  and  $|\tilde{\Psi}_1\rangle_j$ . Consequently, the state  $|\tilde{\Psi}_0\rangle_j$  is an equal superposition of eigenstates  $|\theta_j^\pm\rangle$  of  $U_{P_j}$  with eigenvalues  $e^{\pm i\theta_j}$ , respectively. If it is possible to project onto one of these eigenstates, the standard phase kickback method could be used to encode the phase  $\theta_j$  into a single qubit. A similar approach was considered in Ref. [19]. The CPS method, however, follows a different approach since we are not satisfied with having encoded merely  $\theta_j = \arccos(\tilde{\epsilon}_0|a_j\langle P_j\rangle|)$ . In the end, we wish to have encoded  $\tau_j \cos(\pm\theta_j) = \tilde{\epsilon}_0 a_j\langle P_j\rangle$ . To achieve this, we resort to QSP techniques.

The key insight of QSP is that a sequence of  $n$  single qubit rotations

$$\begin{aligned} \hat{R}_{\phi_n}(\theta) \dots \hat{R}_{\phi_2}(\theta) \hat{R}_{\phi_1}(\theta) \\ = A(\theta)I + iB(\theta)\hat{\sigma}_z + iC(\theta)\hat{\sigma}_x + iD(\theta)\hat{\sigma}_y, \end{aligned} \quad (3)$$

where  $\hat{R}_\phi(\theta) = e^{-i\frac{\theta}{2}(\hat{\sigma}_x \cos \phi + \hat{\sigma}_y \sin \phi)}$  is a discrete single qubit rotation of angle  $\theta$  around a rotation axis specified by  $\phi$  is equivalent to the operation on the left hand side of Eq. (3) where  $A(\theta)$ ,  $B(\theta)$ ,  $C(\theta)$ , and  $D(\theta)$  are polynomials of degree, at most,  $n$ . For our task, it turns out to be sufficient to consider only non-zero polynomials of  $A(\theta)$  and  $C(\theta)$  (see [27] for more details).

The QSP theorem (see Theorem 2 in [28]) states that one can approximate any real odd periodic function  $h(\theta) : (-\pi, \pi] \rightarrow (-\pi, \pi]$  by  $A(\theta), C(\theta)$  being

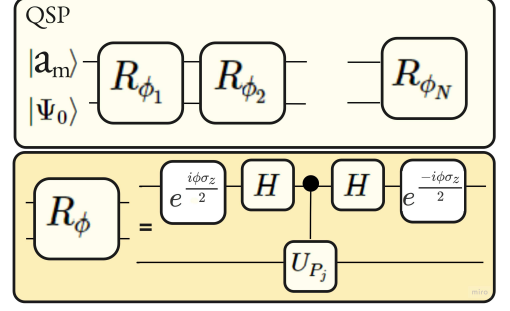


FIG. 2. Quantum circuit realising the QSP by a sequence of controlled unitaries  $\hat{R}_{\phi_i}(\theta)$ ,  $i = 1, \dots, n$ , built from Hadamard gates and controlled  $U_{P_j}$ ,  $|a_m\rangle$  denotes a memory qubit.

Fourier series elements in  $\cos(k\theta)$  and  $\sin(k\theta)$ , respectively ( $k = 0, \dots, n/2$ ) as

$$\max_{\theta \in \mathbb{R}} |A(\theta) + iC(\theta) - e^{ih(\theta)}| \leq \varepsilon_{QSP}. \quad (4)$$

For our purpose, we select  $h(\theta_j) = \tau_j \cos(\theta_j)$  and want to express the functions  $A(\theta_j) = \cos(\tau_j \cos(\theta_j))$ ,  $C(\theta_j) = \sin(\tau_j \cos(\theta_j))$  using a series of single qubit rotations. According to Eq. 3, it is necessary to express  $A$  and  $C$  as polynomial functions. To this end, we use the Jacobi-Anger expansion [29] to rewrite the trigonometric functions as infinite power series. Truncating the series after  $k > n/2$  terms, the error of the approximation of  $e^{i\tau_j \cos \theta_j}$  scales super-exponentially as  $\varepsilon_{QSP} \leq O\left((e\tau_j(2(k+1))^{-1})^{k+1}\right)$ . Using the results of Theorem 3 in Ref. [28], the function  $e^{i\tau_j \cos \theta_j}$  can be simulated with an error  $\varepsilon_{QSP}$  with probability of at least  $1 - 2\varepsilon_{QSP}$  with  $n = O\left(\frac{\log(1/\varepsilon_{QSP})}{\log\log(1/\varepsilon_{QSP})}\right)$  single qubit rotations. The trick to map the QSP approximation of  $e^{i\tau_j \cos \theta_j}$  into the state of the single qubit quantum memory is to perform a controlled version of the single qubit rotation series as depicted in Fig. 2. By doing so the QM state is transformed as  $\alpha|0\rangle + \beta|1\rangle \rightarrow \alpha|0\rangle + e^{i\tau_1 \cos(\theta_1)}\beta|1\rangle$  up to an error of  $\sim \varepsilon_{QSP}$ . Repeating the above procedure for all Pauli strings in the decomposition of  $O$  in a sequential manner, we prepare the QM in a state

$$\begin{aligned} &\approx \frac{1}{\sqrt{2}}(|0\rangle + e^{i\sum_{j=1}^N \tau_j \cos(\theta_j)}|1\rangle) \\ &\approx \frac{1}{\sqrt{2}}(|0\rangle + e^{2i\sqrt{\epsilon}\langle O \rangle}|1\rangle) \end{aligned} \quad (5)$$

up to the QSP simulation errors. At this point, we have ensured, that by CPS method a true estimate of  $\langle O \rangle$  is encoded in the phase of the QM qubit. Note, however, that we have included the factor of  $\sqrt{\epsilon}$  in the encoding. The reason for this is that the phase encoding only provides an estimate of  $\langle O \rangle \bmod 2\pi$ . If we do not know how many multiples of  $2\pi$  comprises  $\langle O \rangle$ , we will not get a

true estimate. This ambiguity is often found in metrology and is referred to as the phase wrapping problem. This brings us to the third and final step of the CPS method.

To control the phase wrapping, we use the *sampling* approach introduced in Refs. [13, 30]. Instead of using fixed  $\epsilon$  to encode  $\theta_j$ , we sample at multiple orders  $\tilde{\epsilon}_l \equiv 2^l \sqrt{\epsilon}$ ,  $l = 1, 2, \dots, d_L$  to gradually enclose on  $\langle O \rangle$ . This can be seen as sequentially estimating the digits of  $\langle O \rangle$ . By a proper selection of  $d_L$  and the number of measurements, we find that the CPS method described above results in an estimate of  $O$  with a variance of  $\sigma^2(\hat{O}_{CPS}) \sim NT^{-1}$ , where  $T$  is the total amount of state preparation circuits ( $V$  and  $V^\dagger$ ) necessary for all steps of the CPS method. The detailed analyses leading to this result can be found in the supplementary material [31].

In Tab. I we compare the required resources for the QEE and CPS method: the coherence time of the required processing ancillas and the number of state preparation circuits. The number of state preparation circuits gives a proper comparison between the two methods that accounts for the added complexity of the CPS method. The costs of  $U_{P_j}$  is in implementation of the controlled sign flip operator  $\Pi_0$  and two state preparation circuits  $\tilde{V}$  and  $\tilde{V}^\dagger$ . The controlled sign flip can, in principle, be decomposed into a number of two-qubit CNOT gates that scales linearly with the number of qubits in the NISQ device [19, 32]. However, access to native multi-qubit controlled gates such as long-range dipole-dipole interactions between Rydberg atoms [33, 34] or photonic cavity-mediated interactions [35] can significantly lower this overhead. We therefore view the most significant overhead as the application of both the state preparation circuit and its inverse.

We also quantify the coherence time in terms of the time needed for running the state preparation circuits,  $t_{prep}$  assuming that this is the most time consuming operation. Consequently, the QEE method only requires a coherence time of the NISQ device of  $\sim t_{prep}$  since after each state preparation the qubits are measured. In comparison, the CPS requires a modest increase in coherence time of the NISQ device that scales logarithmic with the number of Pauli strings and the target precision,  $\eta$ . In return, the CPS method provides a much better estimate of  $\langle O \rangle$  than the QEE method for a fixed number of state preparations. We find that

$$\frac{\sigma^2(\hat{O}_{CPS})}{\sigma^2(\hat{O}_{QEE})} \sim \frac{1}{N}, \quad (6)$$

which shows that the CPS method achieves an Heisenberg-like scaling of the variance in the number of Pauli strings compared to the standard quantum limit scaling of the QEE approach.

Besides the modest increase in coherence time of the NISQ device, the CPS method requires a single auxiliary qubit  $|a_p\rangle$  with a coherence time similar to the NISQ

device and a long-coherence single qubit memory  $|a_m\rangle$  with a coherence time that scales roughly linearly with the number of Pauli strings.

In summary, we have proposed a new method called the *Coherent Pauli Summation* (CPS) method to estimate the expectation values of multi-qubit observables. The method uses QSP techniques to encode information from a multi-qubit processor into a single qubit quantum memory, which allows to overcome the shot noise bottle neck of the conventional QEE approach. Compared to the QEE approach, the CPS method obtains an Heisenberg limited scaling of the estimation precision with the number of Pauli strings in the decomposition of the observable. This represents an improvement of  $1/N$  compared to the QEE approach. We note that this improvement has been estimated assuming that there is on the order of  $N$  non-commuting Pauli strings in the observable decomposition. If there are commuting sets of Pauli strings they can in principle be measured in parallel using the QEE method while the CPS method does not straightforwardly support parallel encoding of commuting Pauli strings. Thus we imagine that potential trade-offs between commuting sets and non-commuting set of Pauli strings can be made resulting in optimal strategies consisting of both the QEE and CPS method depending on the specific observable.

While the CPS method is designed for the estimation of a general observable, we believe that it will, in particular, be relevant for promising NISQ algorithms such as the variational quantum eigensolver where the observable is the energy of the system. In particular for estimating molecular energies where the mapping from a fermionic system to a qubit system often introduces highly non-local terms and large Pauli string representations. For implementation on NISQ devices, we believe that platforms with native multi-qubit controlled gates such as Rydberg atoms [33, 34, 36] or systems with coupling to a common bus mode such as a cavity [35, 37] would be particularly suited due to their potential for implementing the controlled unitaries required for the CPS method.

In the Supplementary materials [31] we discuss a similar method to the CPS method based on Taylor expansion instead of QSP. This method is, however, inferior to the CPS method but we provide it for completeness.

---

\* l.markovich@umail.leidenuniv.nl

† ataalmasi@gmail.com

‡ sinazeytinoglu@hotmail.com

§ J.Borregaard@tudelft.nl

- [1] P. Jurcevic, A. Javadi-Abhari, L.S. Bishop, I. Lauer, D.F. Bogorin, M. Brink, L. Capelluto, O. Günlük, T. Itoko, N. Kanazawa, et al. Demonstration of quantum volume 64 on a superconducting quantum computing system. *Quantum Sci. Technol.*, 6(2):025020, 2021.



Method	Qubits	Coherence times	Number of state preparations
QEE	Processing qubits of NISQ	$t_{prep}$	$N^2/\eta$
CPS	Processing qubits of NISQ	$t_{prep}O(\log(N/\sqrt{\eta}))$	$(N/\eta)O\left(\frac{\log(N/\sqrt{\eta})}{\log \log(N/\sqrt{\eta})}\right)$
	$ a_p\rangle$	$t_{prep}O\left(\frac{\log(N/\sqrt{\eta})}{\log \log(N/\sqrt{\eta})}\right)$	
	$ a_m\rangle$	$Nt_{prep}O\left(\frac{\log(N/\sqrt{\eta})}{\log \log(N/\sqrt{\eta})}\right)$	

TABLE I. Comparison of resources for the QEE approach and the proposed CPS method. In the CPS method,  $|a_p\rangle$  refers to a short coherence time auxiliary qubit required for the encoding step while  $|a_m\rangle$  refers to the long coherence time single qubit quantum memory. We have quantified the necessary coherence times in terms of the state preparation time,  $t_{prep}$ , which is assumed to be the dominant timescale. The observable is assumed to be decomposed into a summation of  $N$  Pauli strings and  $\eta$  is the target precision of the estimation of  $\langle O \rangle$ .

- [2] M. Kjaergaard, M.E. Schwartz, J. Braumüller, P. Krantz, J. Wang, S. Gustavsson, and W.D. Oliver. Superconducting qubits: Current state of play. *Annu. Rev. Condens. Matter Phys.*, 11:369–395, 2020.
- [3] L. Henriët, L. Beguin, A. Signoles, T. Lahaye, A. Browaeys, G.-O. Reymond, and C. Jurczak. Quantum computing with neutral atoms. *Quantum*, 4:327, 2020.
- [4] H. Levine, A. Keesling, G. Semeghini, A. Omran, T.T. Wang, S. Ebadi, H. Bernien, M. Greiner, V. Vuletic, H. Pichler, and M.D. Lukin. Parallel implementation of high-fidelity multiqubit gates with neutral atoms. *Phys. Rev. Lett.*, 123:170503, Oct 2019.
- [5] K.R. Brown, J. Kim, and C. Monroe. Co-designing a scalable quantum computer with trapped atomic ions. *npj Quantum Inf.*, 2(1):1–10, 2016.
- [6] V.M. Schäfer, C.J. Ballance, K. Thirumalai, L.J. Stephenson, T.G. Ballance, A.M. Steane, and D.M. Lucas. Fast quantum logic gates with trapped-ion qubits. *Nature*, 555(7694):75–78, 2018.
- [7] A. Risinger, D. Lobser, A. Bell, C. Noel, L. Egan, D. Zhu, D. Biswas, M. Cetina, and C. Monroe. Characterization and control of large-scale ion-trap quantum computers. *Bull. Am. Phys. Soc.*, 66, 2021.
- [8] R. Babbush, N. Wiebe, J. McClean, J. McClain, H. Neven, and G. K.-L. Chan. Low-depth quantum simulation of materials. *Phys. Rev. X*, 8:011044, Mar 2018.
- [9] Dayou Yang, Andrey Grankin, Lukas M. Sieberer, Denis V. Vasilyev, and Peter Zoller. Quantum non-demolition measurement of a many-body hamiltonian. *Nat. Commun.*, 11(1):775, Feb 2020.
- [10] Edward Farhi, Jeffrey Goldstone, Sam Gutmann, and Leo Zhou. The Quantum Approximate Optimization Algorithm and the Sherrington-Kirkpatrick Model at Infinite Size. *Quantum*, 6:759, July 2022.
- [11] S. McArdle, S. Endo, A. Aspuru-Guzik, S.C. Benjamin, and X. Yuan. Quantum computational chemistry. *Rev. Mod. Phys.*, 92:015003, Mar 2020.
- [12] A. Yu. Kitaev. Quantum measurements and the abelian stabilizer problem. *Conference*, 1995.
- [13] S. Kimmel, G.H. Low, and T.J. Yoder. Robust calibration of a universal single-qubit gate set via robust phase estimation. *Phys. Rev. A*, 92:062315, 2015.
- [14] E. van den Berg. Iterative quantum phase estimation with optimized sample complexity. In *2020 IEEE International Conference on Quantum Computing and Engineering (QCE)*, pages 1–10, 2020.
- [15] H. Mohammadbagherpoor, Y.H. Oh, P. Dreher, A. Singh, X. Yu, and A.J. Rindos. An improved implementation approach for quantum phase estimation on quantum computers. In *2019 IEEE International Conference on Rebooting Computing (ICRC)*, pages 1–9. IEEE, 2019.
- [16] N. Wiebe and C. Granade. Efficient bayesian phase estimation. *Phys. Rev. Lett.*, 117:010503, Jun 2016.
- [17] T.E. O’Brien, B. Tarasinski, and B.M. Terhal. Quantum phase estimation of multiple eigenvalues for small-scale (noisy) experiments. *New J. Phys.*, 21(2):023022, feb 2019.
- [18] A. Peruzzo, J. McClean, P. Shadbolt, M.-H. Yung, X.-Q. Zhou, P.J. Love, A. Aspuru-Guzik, and J.L. O’Brien. A variational eigenvalue solver on a photonic quantum processor. *Nat. Commun.*, 5, 2014.
- [19] D. Wang, O. Higgott, and S. Brierley. Accelerated variational quantum eigensolver. *Phys. Rev. Lett.*, 122:140504, Apr 2019.
- [20] I. Hamamura and T. Imamichi. Efficient evaluation of quantum observables using entangled measurements. *npj Quantum Inf.*, 6:2056–6387, 2020.
- [21] O. Crawford, B. Straaten, D. Wang, T. Parks, E. Campbell, and S. Brierley. Efficient quantum measurement of Pauli operators in the presence of finite sampling error. *Quantum*, 5:385, January 2021.
- [22] Charles Derby, Joel Klassen, Johannes Bausch, and Toby Cubitt. Compact fermion to qubit mappings. *Phys. Rev. B*, 104:035118, Jul 2021.
- [23] J. Nys and G. Carleo. Quantum circuits for solving local fermion-to-qubit mappings. *arXiv preprint arXiv:2208.07192*, 2022.
- [24] F. Verstraete and J. I. Cirac. Mapping local hamiltonians of fermions to local hamiltonians of spins. *Journal of Statistical Mechanics: Theory and Experiment*, 2005(09):P09012, sep 2005.
- [25] J. R. McClean, R. Babbush, P. J. Love, and A. Aspuru-Guzik. Exploiting locality in quantum computation for quantum chemistry. *J. Phys. Chem. Lett.*, 5(24):4368–4380, 2014. PMID: 26273989.
- [26] E. Knill, G. Ortiz, and R. D. Somma. Optimal quantum measurements of expectation values of observables. *Phys. Rev. A*, 75:012328, Jan 2007.
- [27] G.H. Low, T.J. Yoder, and I.L. Chuang. Methodology of resonant equiangular composite quantum gates. *Phys. Rev. X*, 6:041067, Dec 2016.
- [28] G.H. Low and I.L. Chuang. Optimal hamiltonian simulation by quantum signal processing. *Phys. Rev. Lett.*, 118:010501, Jan 2017.
- [29] M. Abramowitz and I.A. Stegun. Handbook of mathematical functions. with formulas, graphs, and mathe-

- mathematical tables. *National Bureau of Standards Applied Mathematics Series. e*, 55:953, 1965.
- [30] B.L. Higgins, D.W. Berry, S.D. Bartlett, M.W. Mitchell, H.M. Wiseman, and G.J. Pryde. Demonstrating heisenberg-limited unambiguous phase estimation without adaptive measurements. *New J. Phys.*, 11(7):073023, jul 2009.
- [31] Supplemental Material:. Appendix a. introduction the new variation of phase-kick back method. appendix b. preparation of  $|\tilde{\Psi}_0\rangle$  state. appendix c. overview of the result known for kitaev qpe. appendix d-h. taylor based variation of the method. appendix i. qsp based variation of the method., 2022.
- [32] D. Maslov. Advantages of using relative-phase toffoli gates with an application to multiple control toffoli optimization. *Phys. Rev. A*, 93:022311, Feb 2016.
- [33] J.T. Young, P. Bienias, R. Belyansky, A.M. Kaufman, and V. Gorshkov. Asymmetric blockade and multiqubit gates via dipole-dipole interactions. *Phys. Rev. Lett.*, 127:120501, Sep 2021.
- [34] D.V. Vasilyev, A. Grankin, M.A. Baranov, L.M. Sieberer, and P. Zoller. Monitoring quantum simulators via quantum nondemolition couplings to atomic clock qubits. *PRX Quantum*, 1:020302, Oct 2020.
- [35] J. Borregaard, P. Kómár, E. M. Kessler, A. S. Sørensen, and M. D. Lukin. Heralded quantum gates with integrated error detection in optical cavities. *Phys. Rev. Lett.*, 114:110502, Mar 2015.
- [36] G. Pelegri, A.J. Daley, and J.D. Pritchard. High-fidelity multiqubit rydberg gates via two-photon adiabatic rapid passage. *Quantum Sci. Technol.*, 7(4):045020, 2022.
- [37] P.-J. Stas, Y. Q. Huan, B. Machielse, E. N. Knall, A. Suleymanzade, B. Pingault, M. Sutula, S. W. Ding, C. M. Knaut, D. R. Assumpcao, Y.-C. Wei, M. K. Bhaskar, R. Riedinger, D. D. Sukachev, H. Park, M. Lončar, D. S. Levonian, and M. D. Lukin. Robust multi-qubit quantum network node with integrated error detection. *Science*, 378(6619):557–560, 2022.

## Appendix

The supplementary materials are organized as follows. In Sec. we introduce the new variation of phase-kick back method of encoding the sum of the mean values of the Pauli strings in the phase. In Sec. the preparation of  $|\tilde{\Psi}_0\rangle$  state is provided. In Sec. we briefly overview the result known for Kitaev QPE to obtain the amount of measurements needed to guarantee the desired precision of the phase estimation. In Sec. we estimate the amount of measurements needed to check that  $\langle P \rangle$  is away from 0 and 1. In Sec. we discuss the  $\text{sign}(\phi)$  estimation. In Sec. the variance of the estimate done by the Taylor based method is provided and in Sec. the error correction procedure is discussed. Next, in Sec. our method is compared with the QEE. In Sec. the phase wrapping problem for the Taylor based method is studied. In Sec. the QSP based variation on the method is provided. In Sec. the phase wrapping control method for Taylor/QSP based method is introduced.

### Phase Kick-back and Taylor Based Variation of our Method

Let us start from the state  $|\Psi_0\rangle$  that can be written as a superposition of two basis states

$$|\Psi_0\rangle = \frac{1}{\sqrt{2}}(|\phi^+\rangle + |\phi^-\rangle), \quad (7)$$

constructed by unitary operator  $V$  such, that applied to the ground state, provides  $V|0\rangle = |\Psi_0\rangle$ . Using the Pauli string operator  $\hat{P}$ , we can introduce

$$|\Psi_1\rangle \equiv \hat{P}|\Psi_0\rangle = \frac{1}{\sqrt{2}}(|\phi^+\rangle + e^{i\phi_0}|\phi^-\rangle), \quad (8)$$

where  $\phi_0$  is an angle that depends on  $P$  action. The product of two states can be written as follows

$$|\langle\Psi_0|\Psi_1\rangle| = |\langle\Psi_0|P|\Psi_0\rangle| = \cos(\phi_0/2). \quad (9)$$

Then the angle  $\phi_0$  is given by

$$\phi_0 = 2 \arccos |\langle\Psi_0|P|\Psi_0\rangle|. \quad (10)$$

Using  $V$  operator and the selective sigh operator  $\Pi_0 = I - 2|0\rangle\langle 0|$  of the ground state, the following operator can be introduced

$$(U)_P = (I - 2|\Psi_0\rangle\langle\Psi_0|)P = (V\Pi_0V^\dagger)P. \quad (11)$$

This unitary operator rotates by a principal angle  $\phi \equiv \phi_0/2$  the closed subspace  $|\Psi_0\rangle$  towards  $|\Psi_1\rangle$  in a Hilbert space. Since the state  $|\Psi_0\rangle$  is (7), where  $|\phi^\pm\rangle$  are the eigenstates of  $U_P$  with eigenvalues  $e^{\pm i\phi}$ , we can retrieve the information

about the mean value of the Pauli string in the phase  $\phi$ , applying  $U_{P_j}$  to  $|\Psi_0\rangle$  and encoding in the quantum memory (QM) qubit the state of the form  $(|0\rangle + e^{i\phi}|1\rangle)/\sqrt{2}$ .

Let us start with Pauli string ( $P_1$ ). Applying  $U_{P_1}$  to the state  $|\Psi_0\rangle$  we encode the state  $(|0\rangle + e^{i\phi_1}|1\rangle)/\sqrt{2}$  in the memory qubit. For the second Pauli string  $P_2$  we reprepare the state  $|\Psi_0\rangle$  and apply  $U_{P_2}$  to encode in  $(|0\rangle + e^{i(\phi_1+\phi_2)}|1\rangle)/\sqrt{2}$  in the QM. Sequentially applying the series of  $N$  encodings, we accumulate  $(|0\rangle + e^{i\sum_{j=1}^N \phi_j}|1\rangle)/\sqrt{2}$  in the memory qubit. However, we can't use this encoding method directly, since the accumulated phase corresponding to the sum of the Pauli strings is

$$\sum_{j=1}^N \phi_j = \sum_{j=1}^N \arccos(|\langle\Psi_0|P_j|\Psi_0\rangle|), \quad (12)$$

that does not take into account the weights  $a_j$  of every Pauli string in the decomposition of the target observable  $O$ . Also, the sum of  $\arccos(\cdot)$  functions is not invertible, so we can not find the target  $\langle O \rangle$ , using the estimate of  $\sum_{j=1}^N \phi_j$ .

To overcome the mentioned difficulties we introduce the state

$$(\sqrt{1-\epsilon'}|0\rangle + \sqrt{\epsilon'}|1\rangle)|\Psi_0\rangle, \quad (13)$$

depending from a parameter  $\epsilon' \in (0, 1)$ . Acting on (13) with a unitary operator  $CP \equiv |0\rangle\langle 0|I + |1\rangle\langle 1|cP$ , where  $I$  is an identity operator and  $cP$  is a controlled Pauli operator, we get the following  $\epsilon'$ -dependent state

$$|\tilde{\Psi}_0\rangle \equiv \sqrt{1-\epsilon'}|0\rangle|\Psi_0\rangle + \sqrt{\epsilon'}|1\rangle|\Psi_1\rangle. \quad (14)$$

Let us also introduce the state

$$|\tilde{\Psi}_1\rangle \equiv (\sigma_x \otimes I)|\tilde{\Psi}_0\rangle. \quad (15)$$

We can immediately write their product as follows

$$\langle\tilde{\Psi}_0|\tilde{\Psi}_1\rangle = 2\sqrt{\epsilon'(1-\epsilon')}\langle\Psi_0|\Psi_1\rangle \quad (16)$$

and see that it contains the mean value of Pauli string multiplied by the  $\epsilon'$ -dependent root.

Thus to encode the sum of the mean values of the Pauli strings to one phase we must use the rotation operator  $(\tilde{U})_{P_j}$ , defined similarly to (11), however, dependent on the preparation circuit  $\tilde{V}(P) : \tilde{V}(P)|0\rangle = |\tilde{\Psi}_0\rangle$  (see Appendix. ). To encode the weighted sum of the Pauli strings we select  $\sqrt{\epsilon'_j(1-\epsilon'_j)} \equiv |a_j|\sqrt{\epsilon}$ , where  $a_j \in \mathbb{R}$  are the coefficients of the Pauli strings decomposition of  $O$  and the parameter  $\epsilon \in (0, 1)$ , holds. After  $N$  encodings the total accumulated phase of the state in the memory qubit is the following

$$\Phi_N = \sum_{j=1}^N \arccos(2\sqrt{\epsilon}|a_j|\langle P_j \rangle). \quad (17)$$

For  $\epsilon \ll 1$ , the Taylor expansion is used to rewrite (17) and, rejecting the  $O$ -big term, we can write:

$$O^\epsilon \equiv \sum_{j=1}^N |a_j|\langle P_j \rangle \approx \frac{N\pi - 2\Phi_N}{4\sqrt{\epsilon}}. \quad (18)$$

Thereby, we can estimate  $O$ , using the estimate of the accumulated phase  $\Phi_N$ .

The encoding method requires preparation of the eigenstate  $|\phi^\pm\rangle$  at each iteration. Since the state  $|\Psi_0\rangle$  is in equal superposition of  $|\phi^\pm\rangle$ , we need to correctly select the encoding operator, applying  $U_{P_j}$  to  $|\phi^+\rangle$  and  $U_{P_j}^\dagger$  to  $|\phi^-\rangle$ . Otherwise, we loose the correct sign of every Pauli an will accumulate them with an error. That is why we need to do several rounds of the quantum phase estimation (QPE) algorithms, to collapse  $|\Psi_0\rangle$  into one of the eigenstates  $|\phi^\pm\rangle$  before the encoding step (see Appendix. for more details).

It is important to mention, that we can write  $|\tilde{\Psi}_0\rangle$  and  $|\tilde{\Psi}_1\rangle$  as the following superposition:

$$|\tilde{\Psi}_0\rangle = \frac{1}{\sqrt{2}}(|\tilde{\phi}_0^+\rangle + |\tilde{\phi}_0^-\rangle), \quad |\tilde{\Psi}_1\rangle = \frac{1}{\sqrt{2}}(|\tilde{\phi}_1^+\rangle + |\tilde{\phi}_1^-\rangle), \quad (19)$$

where we introduce the notations

$$|\tilde{\phi}_0^+\rangle \equiv (\sqrt{1-\epsilon'}|0\rangle + \sqrt{\epsilon'}|1\rangle)|\phi^+\rangle, \quad |\tilde{\phi}_0^-\rangle \equiv (\sqrt{1-\epsilon'}|0\rangle + \sqrt{\epsilon'}e^{i\phi}|1\rangle)|\phi^-\rangle, \quad (20)$$

$$|\tilde{\phi}_1^+\rangle \equiv (\sqrt{1-\epsilon'}|1\rangle + \sqrt{\epsilon'}|0\rangle)|\phi^+\rangle, \quad |\tilde{\phi}_1^-\rangle \equiv (\sqrt{1-\epsilon'}|1\rangle + \sqrt{\epsilon'}e^{i\phi}|0\rangle)|\phi^-\rangle. \quad (21)$$

Hence, projecting on  $|\tilde{\phi}_{0,1}^+\rangle$  and  $|\tilde{\phi}_{0,1}^-\rangle$  is equivalent to projecting on  $|\phi^+\rangle$  and  $|\phi^-\rangle$ , respectively. Thereby, we can use the unitary rotation operators  $(U)_{P_j}$ , introduced in (11) for the QPE step, to resolve between  $|\phi^+\rangle$  and  $|\phi^-\rangle$ .

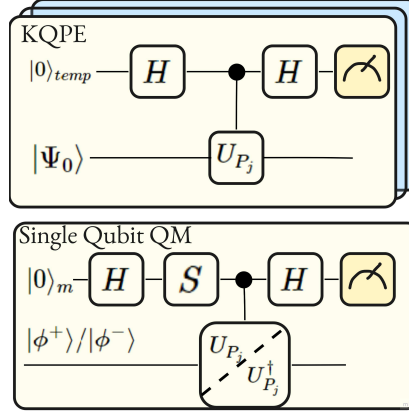


FIG. 3. Quantum circuit proceeding the Kitaev's QPE  $n_{QPE}$  steps on  $|\Psi_0\rangle$  to resolve between  $|\phi^+\rangle$  and  $|\phi^-\rangle$  and the phase-kick back process, encoding the mean values of the Pauli strings in the phase of the state stored in the memory qubit.  $S$  is identity or  $R_z(\pi/2)$  gate.

### $|\tilde{\Psi}_0\rangle$ Preparation

An important step in our algorithm is the  $|\tilde{\Psi}_0\rangle$  state preparation operator  $\tilde{V}(P)|0\rangle = |\tilde{\Psi}_0\rangle$ . Let us select the unitary operator, defined by the following matrix

$$U_\epsilon = \begin{pmatrix} \sqrt{1-\epsilon'} & -\sqrt{\epsilon'} \\ \sqrt{\epsilon'} & \sqrt{1-\epsilon'} \end{pmatrix}, \quad \epsilon' \in (0, 1). \quad (22)$$

Acting with the later operator on the processing ancilla in the ground state, we get

$$U_\epsilon|0\rangle = \sqrt{1-\epsilon'}|0\rangle_p + \sqrt{\epsilon'}|1\rangle_p. \quad (23)$$

Acting with the controlled unitary  $CP$  operator on the state  $|\Psi_0\rangle$ , where  $\sqrt{1-\epsilon'}|0\rangle_p + \sqrt{\epsilon'}|1\rangle_p$  is the control state, we get

$$CP(\sqrt{1-\epsilon'}|0\rangle_p + \sqrt{\epsilon'}|1\rangle_p)|\Psi_0\rangle = \sqrt{1-\epsilon'}|0\rangle_p|\Psi_0\rangle + \sqrt{\epsilon'}|1\rangle_p P|\Psi_0\rangle \equiv |\tilde{\Psi}_0\rangle. \quad (24)$$

### Kitaev's QPE

One of the methods to estimate the phase  $\phi$  of the state is introduced by Kitaev [12]. We will not go into the details of the method, as it is widely described in the literature. The quantum circuit for a standard Kitaev method is shown in Fig. 3 (see [15] for details).

The output state of this circuit with  $K = I$  can be written as follows

$$\frac{1}{2}((1 + e^{i\phi})|0\rangle_p + (1 - e^{i\phi})|1\rangle_p)|\tilde{\Psi}_0\rangle. \quad (25)$$

The probability of measuring  $|0\rangle$  and  $|1\rangle$  are:

$$P(X = 0|\phi) = \frac{1}{2}(1 + \cos(\phi)), \quad P(X = 1|\phi) = \frac{1}{2}(1 - \cos(\phi)), \quad (26)$$

that gives a precise estimates of the modulus of the phase for a sufficient amount of iterations. However, *cosine* does not allow us to distinguish between  $\phi$  and  $-\phi$ . Hence, the same Hadamard test is used, but with  $K = S$ , namely:

$$\frac{1}{2}((1 + ie^{i\phi})|0\rangle_p + (1 - ie^{i\phi})|1\rangle_p)|\tilde{\Psi}_0\rangle. \quad (27)$$



The probabilities of measuring  $|0\rangle$  and  $|1\rangle$  are:

$$P(Y = 0|\phi) = \frac{1}{2}(1 - \sin(\phi)), \quad P(Y = 1|\phi) = \frac{1}{2}(1 + \sin(\phi)), \quad (28)$$

respectively. Repeated measurements of these quantum circuits allow to approximate  $P(X = 0|\phi)$ ,  $P(Y = 0|\phi)$  from which the *sine* and *cosine* values and then the  $\phi$  itself can be estimated. We denote the estimates of  $\sin(\phi)$  and  $\cos(\phi)$  by  $\hat{s}$  and  $\hat{c}$ , respectively. The *tangent* function is more robust to error than the inverse *sine* and *cosine* functions. We write the estimate as follows:

$$\hat{\phi} = \arctan\left(\frac{\hat{s}}{\hat{c}}\right). \quad (29)$$

Since we have two outcomes (0 and 1), we get a Bernoulli distributed independently identically distributed (i.i.d.) sample with probability of success  $P(0|\phi)$ . The probability terms are estimated by frequency  $\hat{\nu}$  to accuracy:

$$|\hat{\nu} - P(0|\phi)| < \epsilon_0. \quad (30)$$

It is straightforward to verify that

$$|\hat{s} - \sin(\phi)| \leq 2\epsilon_0, \quad |\hat{c} - \cos(\phi)| \leq 2\epsilon_0, \quad (31)$$

hold. We want to estimate our angle with high precision, namely

$$|\phi - \arctan\left(\frac{\hat{s}}{\hat{c}}\right)| \leq \epsilon_{tan}. \quad (32)$$

To find the connection between  $\epsilon_{tan}$  and  $\epsilon_0$ , we consider the case  $|\hat{s} - \sin(\phi)| = 2\epsilon_0$ ,  $|\hat{c} - \cos(\phi)| = 2\epsilon_0$  when  $\phi = 0$ . Substituting it in Eq. (32), we get the following bound:

$$\epsilon_0 \leq \frac{\tan(\epsilon_{tan})}{2(1 \mp \tan(\epsilon_{tan}))}. \quad (33)$$

Since in [12]  $\epsilon_{tan} = 1/16$ , holds, we can conclude that  $\epsilon_0 < 1/2(1 - 1/\sqrt{2})$ , holds. To estimate the amount of measurements we need to guaranty Eq. (30), we use Chernoff's inequality (see for example [14]):

$$1 - 2\exp(-2n_0\epsilon_0^2) \leq P(|\hat{\nu}_0 - P(0|\phi)| < \epsilon_0). \quad (34)$$

In many applications, it is important to know what the sample size must be in order that, with probability at least  $(1 - \eta_0)$ , one could assert that the estimate differ from the corresponding value by an amount less than  $\epsilon_0$ . In other words, beginning with what value  $n_0$ , does the following inequality  $2\exp(-2n_0\epsilon_0^2) \leq \eta_0$ ,  $\eta_0 \in [0, 1]$ , holds? One can deduce that the amount of measurements that guarantee this is equal to:

$$n_0 \geq \frac{\log(2/\eta_0)}{2\epsilon_0^2}. \quad (35)$$

Taking into account that each Hadamard test has to be done twice and  $m$  angle estimations are done to get enough statistical samples, we get in total  $2m$  estimations. Hence, in total we do

$$M_K \geq \frac{m \log(2/\eta_0)}{\epsilon_0^2}. \quad (36)$$

One can see, that due to the *sine* and *cosine* functions the method performs bad in the boundary points of 0 and 1. That is why we need to do a preliminary check that every  $\langle P_j \rangle$  is in the interval bounded away from 0 and 1 done by a small amount of projective measurements.

### On Selecting the Amount of Protective Measurements for the Boundary Condition Check-up

We use the method introduced in [19]. Let  $\hat{A}$  be an estimate of  $A \equiv \langle P \rangle$ , using  $n_1$  samples. For the independent random variables bounded by the interval  $[0, 1]$  the Hoeffding's inequality:

$$P(|A - \hat{A}| \geq g_1) \leq 2 \exp(-2n_1 g_1^2), \quad (37)$$

holds, where  $g_1 > 0$ . The parameters  $g_1$  and  $n_1$  can be selected according to our needs of the estimation precision.

Since we need to collapse  $|\tilde{\Psi}_0\rangle$  into one of the states  $|\phi^\pm\rangle$  with high confidence, we have to bound  $A$  away from 0 and 1 by a constant. Thereby, we would like  $A \in I = [0 + \delta, 1 - \delta]$ . Reversing Eq. (37), we get:

$$1 - 2 \exp(-2n_1 g_1^2) \leq P(|A - \hat{A}| < g_1). \quad (38)$$

We deduce that

$$2 \exp(-2n_1 g_1^2) \leq \eta_1, \quad (39)$$

holds, where  $\eta_1 \in [0, 1]$  is the desired probability of being inside of  $A \in I$ . The total amount of projective measurements we need for  $N$  Paulis is  $M_1 = Nn_1$ .

### On $\text{sign}(\phi)$ Estimation

In the previous section we selected  $n_1$  in such a way that with  $1 - \eta_1$  probability  $A$  is in  $I$ . Using the part of Kitaev's QPE circuit whose action is given by Eq. (27), we find that the probability of measuring  $|0\rangle$  and  $|1\rangle$  is given by Eq. (28). If  $\phi_0 > 0$  the probability  $P(Y = 0|\phi_0) < 1/2$ , holds. We will use this fact to find out the  $\text{sign}(\phi)$ .

Since  $\phi_0 = 2 \arccos(|A|)$  we can write:

$$\begin{aligned} P(Y = 0|\phi_0) &= \frac{1}{2}(1 - \sin \phi_0) \in [p_{0min}, p_{0max}], \quad \text{where} \\ p_{0min} &= \frac{1}{2}(1 - \sin(2 \arccos(|1 - \delta|))), \quad p_{0max} = \frac{1}{2}(1 - \sin(2 \arccos(|\delta|))), \quad \text{if } \delta < 1/2, \end{aligned} \quad (40)$$

and

$$\begin{aligned} P(Y = 1|\phi_0) &= \frac{1}{2}(1 + \sin \phi_0) \in [p_{1min}, p_{1max}], \quad \text{where} \\ p_{1min} &= \frac{1}{2}(1 + \sin(2 \arccos(|\delta|))), \quad p_{1max} = \frac{1}{2}(1 + \sin(2 \arccos(|1 - \delta|))), \quad \text{if } \delta < 1/2. \end{aligned} \quad (41)$$

For example, if we select  $\delta = 0.2$  then the probabilities are defined on the distant intervals  $P(Y = 0|\phi_0) \in [0.02, 0.3]$ ,  $P(Y = 1|\phi_0) \in [0.7, 0.98]$ . Thus, for the reasonable selection of  $\delta$  the probabilities are spaced apart from  $1/2$ .

Since our goal is to find  $P(Y = 0|\phi_0) \leq 1/2$ , we use the Hoeffding's inequality with the following conditions:

$$1 - 2 \exp(-2g_3^2(\delta)n_{QPE}) \leq P(|\hat{\nu}_{Y=0} - P(Y = 0|\phi_0)| < g_3(\delta)), \quad (42)$$

where  $g_3(\delta) \equiv \frac{1}{2} - p_{0max}(\delta)$  and  $\hat{\nu}_{Y=0}$  is a frequency of the event  $Y = 0$ . Beginning with what value  $n_{QPE}$ , we would like that

$$2 \exp(-2g_3^2(\delta)n_{QPE}) \leq \eta_3, \quad \eta_3 \in [0, 1], \quad (43)$$

holds? [ata]. One can deduce that it is bounded as follows

$$n_{QPE} \geq \frac{\log(2/\eta_3)}{2g_3^2(\delta)}. \quad (44)$$

Since we run the algorithm for  $N$  phases, we get the total amount of QPE rounds bounded by

$$M_{QPE} \geq \frac{N \log(2/\eta_3)}{2g_3^2(\delta)}. \quad (45)$$

Finally, setting  $M_{QPE}$  with probability  $1 - \eta_3$  we will estimate  $P(Y = 0|\phi)$  by  $\hat{\nu}_{Y=0}$  with enough precision to determine  $P(Y = 0|\phi) \leq \frac{1}{2}$ .

### Variance of the Taylor Based Method

After the sign estimation done by  $n_{QPE}$  rounds of QPE we do the phase encoding in the memory qubit  $|a_m\rangle = |+\rangle$ , applying  $\tilde{U}_P$  or  $\tilde{U}_P^\dagger$ . This process is repeated  $N$  times until all the phases connected with the Pauli strings are encoded in the long coherence time QM. The accumulated state encoded in  $|a_m\rangle$  is

$$|\Phi_N\rangle = \frac{|0\rangle + e^{i\Phi_N}|1\rangle}{\sqrt{2}}|\phi_1\rangle|\phi_2\rangle\cdots|\phi_N\rangle, \quad \Phi_N = \sum_{i=1}^N \arccos(2\sqrt{\epsilon}|a_j\rangle\langle P_j|). \quad (46)$$

Then we apply the Hadamart gate

$$H \otimes I |\Phi_N\rangle = \frac{(1 + e^{i\Phi_N})|0\rangle + (1 - e^{i\Phi_N})|1\rangle}{2}|\phi_1\rangle|\phi_2\rangle\cdots|\phi_N\rangle. \quad (47)$$

Similarly to the previous sections, the probabilities to measure  $|0\rangle$  and  $|1\rangle$  are

$$P(X = 0|\Phi_N) = \frac{1}{2}(1 + \cos(\Phi_N)), \quad P(X = 1|\Phi_N) = \frac{1}{2}(1 - \cos(\Phi_N)). \quad (48)$$

If we act on  $|a_m\rangle$  with  $S$  gate and then do encoding, after all steps we get

$$|\Phi_N\rangle = \frac{|0\rangle + ie^{i\Phi_N}|1\rangle}{\sqrt{2}}|\phi_1\rangle|\phi_2\rangle\cdots|\phi_N\rangle. \quad (49)$$

Then we apply the Hadamart gate and get the state

$$H \otimes I |\Phi_N\rangle = \frac{(1 + ie^{i\Phi_N})|0\rangle + (1 - ie^{i\Phi_N})|1\rangle}{2}|\phi_1\rangle|\phi_2\rangle\cdots|\phi_N\rangle \quad (50)$$

and the probabilities to measure  $|0\rangle$  and  $|1\rangle$  are

$$P(Y = 0|\Phi_N) = \frac{1}{2}(1 + \sin(\Phi_N)), \quad P(Y = 1|\Phi_N) = \frac{1}{2}(1 - \sin(\Phi_N)). \quad (51)$$

Since we don't know the preparation circuit of the state  $|\Phi_N\rangle$ , we can't use QPE to estimate the phase directly. To approximate  $P(X = 0|\Phi_N)$ ,  $P(Y = 0|\Phi_N)$  and then estimate the total accumulated phase we need to repeat all the procedure of encoding  $M_q$  times, every time doing the projective measurement on the state encoded in the QM. Then, using the probability estimates, we estimate *sine* and *cosine* that will determine the estimate of  $\Phi_N$ . To this end, we introduce the notation

$$\hat{Q} \equiv \frac{1 - 2\hat{P}(Y = 0|\Phi_N)}{2\hat{P}(X = 0|\Phi_N) - 1} = \hat{\tan}(\Phi_N), \quad (52)$$

and the variance of the estimate of  $\Phi_N$  is the following

$$\sigma^2 \hat{\Phi}_N \approx \left( \frac{\partial \Phi_N}{\partial Q} \right)^2 \sigma^2 \hat{Q} = \left( \frac{1}{1 + Q^2} \right)^2 \sigma^2 \hat{Q}. \quad (53)$$

The variance of  $Q$  can be written as follows

$$\sigma^2 \hat{Q} \approx \sigma^2 \hat{P}(X = 0|\Phi_N) \left( \frac{2(1 - 2\hat{P}(Y = 0|\Phi_N))}{(2\hat{P}(X = 0|\Phi_N) - 1)^2} \right)^2 + \sigma^2 \hat{P}(Y = 0|\Phi_N) \left( \frac{2}{2\hat{P}(X = 0|\Phi_N) - 1} \right)^2. \quad (54)$$

Since we have a Bernoulli distribution, the variances are

$$\sigma^2 \hat{P}(X = 1|\Phi_N) = \frac{\hat{P}(X = 0|\Phi_N)\hat{P}(X = 1|\Phi_N)}{M_q}, \quad \sigma^2 \hat{P}(Y = 1|\Phi_N) = \frac{\hat{P}(Y = 0|\Phi_N)\hat{P}(Y = 1|\Phi_N)}{M_q}, \quad (55)$$

where  $M_q$  is the amount of repetitions of  $|\Phi_N\rangle$ . Finally, the variance (53) is the following:

$$\sigma^2 \hat{\Phi}_N \approx \frac{3 + \cos(8\pi\Phi_N)}{4M_q} \sim \frac{1}{M_q}. \quad (56)$$

Since (18), holds, the variance of the estimate of  $O$  is the following

$$\sigma^2 \hat{O}^\epsilon \approx \left( \frac{\partial O^\epsilon}{\partial \phi} \right)^2 \sigma^2 \hat{\Phi}_N \sim \frac{1}{M_q \epsilon}. \quad (57)$$

### Error Correction

Since we used the Taylor expansion to get rid of *arc-cosine* function in (17), we inserted an error by neglecting the  $O$ -big term. To correct it we use the QEE strategy to estimate the correction terms. Our corrected value is the following

$$\hat{O}_T^{Qcor} = \hat{O}^\epsilon + \frac{1}{2\sqrt{\epsilon}} \sum_{n=1}^{\infty} \frac{(2n)!(2\sqrt{\epsilon})^{2n+1}}{4^n (n!)^2 (2n+1)} \hat{P}_{cor}^{2n+1}, \quad (58)$$

where

$$\hat{P}_{cor}^{2n+1} = \sum_{i=1}^N |a_i^{2n+1} \langle \hat{P}_i \rangle^{2n+1}|, \quad (59)$$

is the sum of the Pauli strings estimates done by the projective measurements (like it is done in QEE method). The variance of the correction term can be straightforwardly written as

$$\sigma^2 P_{cor}^{2n+1} = \frac{(2n+1)}{n_c^{cor}} \sum_{j=1}^N (a_j^{2n+1} \langle P_j \rangle^{2n})^2 (1 - \langle P_j \rangle^2), \quad (60)$$

where  $n_c^{cor}$  is the amount of the projective measurements done for every Pauli string. Then  $M_c^{cor} = N n_c^{cor}$  is the amount of the projective measurement done to estimate  $N$  correction terms. Hence, the variance of the estimate of  $O$  is the following

$$\sigma^2 \hat{O}_T^{Qcor} = \sigma^2 \hat{O}^\epsilon + \frac{1}{n_c^{cor}} \sum_{j=1}^N \sum_{n=1}^{\infty} \frac{((2n)!)^2 2^{4n} \sqrt{\epsilon}^{4n}}{2^{4n} (n!)^4} a_j^{2(2n+1)} \langle P_j \rangle^{4n} (1 - \langle P_j \rangle^2). \quad (61)$$

The series in the right hand side is of the type:

$$\sum_{n=1}^{\infty} \frac{((2n)!)^2 (2\sqrt{\epsilon} a_j \langle P_j \rangle)^{4n}}{2^{4n} (n!)^4} = \frac{2}{\pi} K \left( 16\sqrt{\epsilon}^4 a_j^4 \langle P_j \rangle^4 \right) - 1 \quad \text{if} \quad \sqrt{\epsilon}^2 a_j^2 \langle P_j \rangle^2 < 1/4, \quad (62)$$

where

$$K(t) = \int_0^{\pi/2} \frac{d\theta}{\sqrt{1 - t \sin^2 \theta}}, \quad (63)$$

is the complete elliptic integral of the first kind. One must be careful with the notation when using these functions, because various reputable references and software packages use different conventions in the definitions of the elliptic functions. On Wikipedia  $K(k)$  is used,  $k^2 = t$ , holds. Finally, we can rewrite Eq. (61) as follows

$$\sigma^2 \hat{O}_T^{Qcor} = \frac{1}{\epsilon M_q} + \frac{1}{n_c^{cor}} \sum_{j=1}^N \left[ \frac{2}{\pi} K \left( 16\epsilon^2 a_j^4 \langle P_j \rangle^4 \right) - 1 \right] a_j^2 (1 - \langle P_j \rangle^2), \quad (64)$$

if

$$\epsilon < (4a_j^2 \langle P_j \rangle^2)^{-1}, \quad (65)$$

holds for all  $j = 1, \dots, N$ . Let us use the following asymptotic expression:

$$K(t) \approx \frac{\pi}{2} + \frac{\pi}{8} \frac{t}{1-t} - \frac{\pi}{16} \frac{t^2}{1-t}. \quad (66)$$

This approximation has a relative precision better than  $3 \times 10^{-4}$  for  $t < 1/4$  ( $k < 1/2$ ). Keeping only the first two terms is correct to 0.01 precision for  $t < 1/4$  ( $k < 1/2$ ).

We can conclude that one can use (66) if  $t \equiv \epsilon^2 a_j^4 \langle P_j \rangle^4 < 1/4$ . Since Eq. (65), holds, it is always true. Using this assumption, we can rewrite Eq. (64) as follows:

$$\sigma^2 \hat{O}_T^{Qcor} \sim \frac{1}{\epsilon M_q} + \frac{\epsilon^2}{n_c^{cor}} \sum_{j=1}^N a_j^6 \langle P_j \rangle^4 (1 - \langle P_j \rangle^2). \quad (67)$$

We select  $\epsilon \ll 1$ . Taking the derivative on  $\epsilon$  and equating it to zero, we get the optimal  $\epsilon$  that minimizes the variance (67):

$$\epsilon = \sqrt[3]{\frac{n_c^{cor}}{M_q \sum_{j=1}^N a_j^6 \langle P_j \rangle^4 (1 - \langle P_j \rangle^2)}} \sim \left( \frac{n_c^{cor}}{M_q} \right)^{\frac{1}{3}} \frac{1}{N^{\frac{1}{3}}} = \left( \frac{M_c^{cor}}{M_q} \right)^{\frac{1}{3}} \frac{1}{N^{\frac{2}{3}}}. \quad (68)$$

The standard deviation of our estimate should be bigger or equal to the error value that can be done on the sign estimation and QPE steps, namely  $\sum_{j=1}^N 2a_j \langle P_j \rangle ((1 - \eta_1)\eta_3 + \eta_1/2)$ . The parameters  $\eta_1$  and  $\eta_3$  are defined in (39) and (44) as

$$\eta_1 = \frac{2}{e^{2n_1 g_1^2}}, \quad \eta_3 = \frac{2}{e^{2n_{QPE} g_3^2(\delta)}}. \quad (69)$$

Let us assume  $\eta_1$  being the same rate as  $\eta_3$ . Since  $\eta_1 \ll 1$ , we can write

$$(1 - \eta_1)\eta_3 + \eta_1/2 \sim \eta_3 + \eta_1/2 \sim e^{-2n_{QPE} g_3^2(\delta)}. \quad (70)$$

If we assume that all Paulis are equal with equal weights, then we can write the condition

$$\sigma^2 \hat{O}_T^{Qcor} \geq 36a^2 \langle P \rangle^2 N^2 e^{-4n_{QPE} g_3^2(\delta)}. \quad (71)$$

Finally if we define the target precision  $\sigma^2 \hat{O}_T^{Qcor} = \eta$ , we can conclude

$$n_{QPE} = O\left(\log\left(\frac{N}{\sqrt{\eta}}\right)\right) \quad (72)$$

that gives the scaling of QPE steps required for our method.

### Comparison of Taylor Based Method and QEE Method

In this section we would like to compare the Taylor based variation of our method with the QEE. In QEE every Pauli string is measured independently and then all the results are summed up. Hence, the variance of the estimate of  $O$  is the following:

$$\sigma^2 \hat{O}^{QEE} \equiv \sum_{i=1}^N \frac{a_i^2 \sigma^2 \hat{P}_i}{n_c} = \frac{N}{M_c} \sum_{i=1}^N a_i^2 (1 - \langle \Psi_0 | P_i | \Psi_0 \rangle^2) \sim \frac{N^2}{M_c}, \quad (73)$$

where  $M_c = Nn_c$  is the amount of projective measurements (or controlled unitaries) done in QEE. Then

$$\frac{\sigma^2 \hat{O}_T^{Qcor}}{\sigma^2 \hat{O}^{QEE}} \sim \frac{\frac{1}{M_q^{\frac{2}{3}} (n_c^{cor})^{\frac{1}{3}}} \left( \sum_{j=1}^N a_j^6 \langle P_j \rangle^4 (1 - \langle P_j \rangle^2) \right)^{\frac{1}{3}}}{\frac{1}{n_c} \sum_{j=1}^N a_j^2 (1 - \langle P_j \rangle^2)}. \quad (74)$$



Let us assume that the amount of resources needed for both methods are equal. For our Taylor based method we make  $M_T = M_c^{cor} + M_q(1 + M_{QPE})$ . Hence we select  $M_c = M_T$  and, substituting (68) in (74), we get

$$\frac{\sigma^2 \hat{O}_T^{Qcor}}{\sigma^2 \hat{O}_{QEE}} \sim \frac{M_q(1 + M_{QPE}) + M_c^{cor}}{N^{\frac{2}{3}} M_q^{\frac{2}{3}} (M_c^{cor})^{\frac{1}{3}}} \frac{\left( \sum_{j=1}^N a_j^6 \langle P_j \rangle^4 (1 - \langle P_j \rangle^2) \right)^{\frac{1}{3}}}{\sum_{j=1}^N a_j^2 (1 - \langle P_j \rangle^2)}. \quad (75)$$

Since we are interested in the rate, we assume the case when all  $P_j$  and  $a_j$  are equal for all  $j$ . Then the latter ratio will reduce to

$$\frac{\sigma^2 \hat{O}_T^{Qcor}}{\sigma^2 \hat{O}_{QEE}} \sim \frac{M_q(1 + M_{QPE}) + M_c^{cor}}{N^{\frac{4}{3}} M_q^{\frac{2}{3}} (M_c^{cor})^{\frac{1}{3}}} \frac{\langle P \rangle^{\frac{4}{3}}}{(1 - \langle P \rangle^2)^{\frac{2}{3}}}. \quad (76)$$

Since (72), holds, and  $M_c^{cor} = N m_c^{cor}$ , we can conclude

$$\frac{\sigma^2 \hat{O}_T^{Qcor}}{\sigma^2 \hat{O}_{QEE}} \sim \frac{1}{N^{\frac{2}{3}}}. \quad (77)$$

### Control of Phase Wrapping for the Taylor Based Method

The state (46) encoded in the memory qubit contains the phase

$$\hat{\Phi}_N = \sum_{j=1}^N \arccos(2\sqrt{\epsilon} |a_j \langle P_j \rangle|) \mod 2\pi, \quad (78)$$

accumulated by the  $N$  rounds of encoding. Unfortunately, the phase in our method is estimated only up to modulus  $2\pi$ . With the growth of  $N$  the phase  $\Phi_N \notin [-\pi, \pi)$  and we have no information about how many times  $L$  the phase wraps around  $2\pi$ . If we use the QEE method of the mean value estimation, we can define

$$\hat{\Phi}_{QEE} = \sum_{j=1}^N \arccos(2\sqrt{\epsilon} |a_j \langle (\hat{P}_j)_{QEE} \rangle|) \quad (79)$$

that also can be written as  $\Phi_{QEE} = 2\pi L + \Phi$ . Let the estimate of  $\Phi$  be taken as  $\hat{\Phi}_N$  and, hence, the estimate of  $L$  is

$$\hat{L} = \frac{1}{2\pi} (\hat{\Phi}_{QEE} - \hat{\Phi}_N). \quad (80)$$

The variance of such estimate is

$$\sigma^2 \hat{L} = \frac{1}{4\pi^2} (\sigma^2 \hat{\Phi}_{QEE} + \sigma^2 \hat{\Phi}_N) \sim \frac{\epsilon N^2}{M_c^{cor}} + \frac{1}{M_q}. \quad (81)$$

Using the Chebyshev's inequality, where the estimate of  $L$  is its expectation, for all  $c > 0$ , we can write

$$P(|L - \hat{L}| \geq c) \leq \frac{\sigma^2 \hat{L}}{c^2}. \quad (82)$$

If  $c = 1$  the error inserted in the phase estimation is at least  $2\pi$ . Hence, to have no effect of wrapping we need the standard deviation of our estimate to be bigger or equal to the error value that can be done during the phase wrapping estimation, namely  $\frac{2\pi}{\sqrt{\epsilon}} P(|L - \hat{L}| \geq c)$ . Using (82), we can write

$$\sqrt{\frac{1}{\epsilon M_q} + \frac{N^2 \epsilon^2}{M_c^{cor}}} \geq \frac{2\pi}{\sqrt{\epsilon}} \frac{\sigma^2 \hat{L}}{c^2}. \quad (83)$$

Selecting  $c = 1$  and substituting (81) in (83), we get the following condition

$$M_q \geq 2\pi^2 (N^{\frac{2}{3}} + 1)^2. \quad (84)$$

Hence, using the same  $M_T$  measurements we can control the phase wrapping. However, we got an extra condition (84), namely  $M_q$  scales with  $N^{\frac{4}{3}}$ . However, we can consider another approach to control the phase wrapping in the Taylor based method, eliminating the condition (84), shown in Appendix .

### QSP based method

In [28] the following idea is presented. Let us have a single qubit rotation around  $x$  axes

$$\hat{R}(\theta) = e^{-i\frac{\theta}{2}\hat{\sigma}_x} = \cos\left(\frac{\theta}{2}\right)I + \sin\left(\frac{\theta}{2}\right)\hat{\sigma}_x \quad (85)$$

with an angle  $\theta$ . This rotation is considered as a computational module that computes some unitary function that depends on the selected parameter  $\theta$ , the input state and the measurement basis. If we multiply different rotations together, apply them to a zero state and project onto a zero state, namely  $\langle 0|\hat{R}(\theta) \dots \hat{R}(\theta)\hat{R}(\theta)|0\rangle = \cos(N\theta/2)$ , we compute a cosine function dependent from  $\theta$  parameter. To compute more interesting function a less primitive unitary is introduced

$$\hat{R}_\phi(\theta) = e^{-i\frac{\phi}{2}\hat{\sigma}_z}\hat{R}(\theta)e^{-i\frac{\phi}{2}\hat{\sigma}_z}. \quad (86)$$

A sequence of such  $n$  single qubit rotations

$$\hat{R}_{\phi_n}(\theta) \dots \hat{R}_{\phi_2}(\theta)\hat{R}_{\phi_1}(\theta) = A(\theta)I + iB(\theta)\hat{\sigma}_z + iC(\theta)\hat{\sigma}_x + iD(\theta)\hat{\sigma}_y, \quad (87)$$

with a specific choice of different parameters  $\vec{\phi}$  can compute more general functions of  $\theta$  in terms of  $A(\theta)$ ,  $B(\theta)$ ,  $C(\theta)$ ,  $D(\theta)$ , being the polynomials of, at most, degree  $n$ . Often it is enough to use the partial set of  $(A, B, C, D)$ , for example  $(A, C)$  (see [27] for more details). The following theorem holds

**Theorem .1.** [27] *For any even  $n > 0$ , a choice of real functions  $A(\theta)$ ,  $C(\theta)$  can be implemented by some  $\vec{\phi} \in R^n$  if and only if all these are true:*

- For any  $\theta \in R$ ,

$$A^2(\theta) + C^2(\theta) \geq 1, \quad \text{and} \quad A(0) = 1, \quad (88)$$

- $A(\theta) = \sum_{k=0}^{n/2} a_k \cos(k\theta)$ ,  $\{a_k\} \in R^{n/2+1}$ ,  $C(\theta) = \sum_{k=0}^{n/2} c_k \cos(k\theta)$ ,  $\{c_k\} \in R^{n/2}$ .

Moreover,  $\vec{\phi}$  can be efficiently computed from  $A(\theta)$ ,  $C(\theta)$ .

Given a unitary  $\hat{U}$  with eigenstates  $\hat{U}|\phi\rangle = e^{ih(\theta)}|\phi\rangle$  a quantum circuit  $\hat{V}_{ideal}(\theta) = \sum_{\lambda} e^{ih(\theta)}|\phi\rangle\langle\phi|$  can be constructed, where  $h(\theta)$  is a real function.

**Theorem .2.** (quantum signal processing) *Any real odd periodic function  $h : (-\pi, \pi] \rightarrow (-\pi, \pi]$  and even  $n > 0$ , let  $A(\theta), C(\theta)$  be real Fourier series in  $\cos(k\theta)$ ,  $\sin(k\theta)$ ,  $k = 0, \dots, n/2$ , that approximate*

$$\max_{\theta \in R} |A(\theta) + iC(\theta) - e^{ih(\theta)}| \leq \varepsilon_{QSP}. \quad (89)$$

QSP use just a single ancilla qubit and the query complexity of the methodology is exactly the degree  $n$  of optimal trigonometric polynomial approximations to  $e^{ih(\theta)}$  with error  $\varepsilon_{QSP}$ . It is mentioned, that  $A(\theta)$ ,  $C(\theta)$  satisfying the later theorem, in general, do not satisfy (88). Thus the rescaling is provided

$$\begin{aligned} A_1(\theta) &= A(\theta)/(1 + \varepsilon_{QSP}), \quad C_1(\theta) = C(\theta)/(1 + \varepsilon_{QSP}), \\ |A_1(\theta) + iC_1(\theta) - e^{ih(\theta)}| &\leq \varepsilon_{QSP}/(1 + \varepsilon_{QSP}) + \varepsilon_{QSP} < 2\varepsilon_{QSP}. \end{aligned} \quad (90)$$

Hence, the success probability of the method is at least  $1 - 2\varepsilon_{QSP}$ .

We select  $h(\theta) = \tau \cos(\theta)$  and the input is  $\theta = \arccos(2\sqrt{\epsilon}|a(P)|)$ . Then

$$A(\theta) = \cos(\tau \cos(\theta)), \quad C(\theta) = \sin(\tau \cos(\theta)), \quad (91)$$

hold. We can use the real-valued Jacobi-Anger expansion [29] to rewrite the later functions as series:

$$\begin{aligned} \cos(\tau \cos(\theta)) &\equiv J_0(\tau) + 2 \sum_{m=1}^{\infty} (-1)^m J_{2m}(\tau) \cos(2m\theta), \\ \sin(\tau \cos(\theta)) &\equiv -2 \sum_{m=1}^{\infty} (-1)^m J_{2m-1}(\tau) \cos[(2m-1)\theta], \end{aligned} \quad (92)$$

where  $J_m(\tau)$  is the  $m$ -th Bessel function of the first kind. The Bessel function  $J_m(\tau)$  is bounded, for real  $\tau$  and integer  $n$  as

$$|J_m(\tau)| \leq \frac{1}{|m|!} \left| \frac{\tau}{2} \right|^{|m|}. \quad (93)$$

Under the conditions  $|\tau| \leq k$  and  $l! > (l/e)^l$  we can introduce the upper bound

$$2 \sum_{m=k+1}^{\infty} |J_m(\tau)| \leq 4 \sum_{m=k+1}^{\infty} \frac{1}{|m|!} \left| \frac{\tau}{2} \right|^{|m|} < \frac{4}{(k+1)!} \left| \frac{\tau}{2} \right|^{k+1} < 4 \left| \frac{e\tau}{2(k+1)} \right|^{k+1}. \quad (94)$$

Thus, we can truncate the series (92) at some point  $k > n/2$  and keep the first  $k$  terms. The error of the approximation of every  $e^{i\tau \cos[\arccos(2\sqrt{\epsilon}|a_j\rangle\langle P_j|)]}$ ,  $j = 1, \dots, N$  is scaled super-exponentially as

$$\varepsilon_{QSP} \leq O\left(\left(\frac{e\tau}{2(k+1)}\right)^{k+1}\right), \quad (95)$$

where  $|\tau| \leq k = n/2$ , holds. Taking  $k = e(\tau + \gamma)/2$ , where  $\gamma > 0$  and  $\tau = O(\gamma)$  we get the following amount of qubits [27]:

$$n_{QSP} \equiv n = O\left(\frac{\log(1/\varepsilon_{QSP})}{\log \log(1/\varepsilon_{QSP})}\right). \quad (96)$$

Hence, if the QSP method would approximate the function perfectly, the phase encoded in the memory qubit could be written as

$$\exp(i\phi_j) = \exp(i\tau_j \cos[\arccos(2\sqrt{\epsilon}|a_j\rangle\langle P_j|)]) = \exp(2i\tau_j\sqrt{\epsilon}|a_j\rangle\langle P_j|). \quad (97)$$

To encode correctly the later mean values in the memory qubit, we need to select  $\tau_j = \text{sign}(a_j\langle P_j|)$ . Then the encoding will be with the correct sign of the Pauli string. However, since QSP method is not perfectly approximating the function from the random variable, we have to take into account the error emerging in the  $e^{i\tau \cos(\cdot)}$  QSP approximation:

$$\left| f_{QSP}(\arccos(2\sqrt{\epsilon}|a_j\rangle\langle P_j|)) - \exp(2i\tau_j\sqrt{\epsilon}|a_j\rangle\langle P_j|) \right| < \varepsilon_{QSP}, \quad (98)$$

where  $f_{QSP}$  is the approximation of  $\exp(i\tau \cos(\cdot))$ . Then we can write

$$f_{QSP}(\phi_j) = \exp(i\phi_j) \pm r_j \exp(i\delta_j), \quad (99)$$

where  $|r_j \exp(i\delta_j)| < \varepsilon_{QSP}$ . After  $N$  encodings, we get the final state stored in the memory qubit

$$\begin{aligned} |\Phi_N\rangle &= (|0\rangle + (e^{i\phi_1} + r_1 e^{i\delta_1})(e^{i\phi_2} + r_2 e^{i\delta_2}) \dots (e^{i\phi_N} + r_N e^{i\delta_N})|1\rangle) |\phi_1^N\rangle \\ &= \left( |0\rangle + \left( e^{i\Phi_N} + \sum_{j=1}^N r_j e^{i\delta_j} e^{i \sum_{k=1, k \neq j}^N \phi_k} + \sum_{\substack{j,k=1, \\ j \neq k}}^N r_j r_k e^{i(\delta_j + \delta_k)} e^{i \sum_{r=1, r \neq j, k}^N \phi_r} + \dots + (r_1 r_2 \dots r_N) e^{i \sum_{j=1}^N \delta_j} \right) |1\rangle \right) |\phi_1^N\rangle. \end{aligned} \quad (100)$$

where we used the notations  $|\phi_1^N\rangle \equiv |\phi_1\rangle|\phi_2\rangle \dots |\phi_N\rangle$ ,  $\Phi_N = \sum_{j=1}^N \phi_j$ . Let all  $r_j$  and  $\delta_j$  be equal. The series on the right hand side can be always written as

$$C_N^1 r e^{i\delta} e^{i \sum_{k=1, k \neq 1}^N \phi_k} + C_N^2 r^2 e^{2i\delta} e^{i \sum_{r=1, r \neq 1, 2}^N \phi_r} + \dots + C_N^N r^N e^{iN\delta} = R e^{i\Theta_R}, \quad (101)$$

$$R = \sqrt{\sum_{j=1}^N (C_N^j r^j)^2 + 2 \sum_{j,k=1, j \neq k}^N C_N^j C_N^k r^j r^k \cos\left(i \left( (j-k)\delta + \sum_{r=1, r \neq j}^N \phi_r - \sum_{r=1, r \neq k}^N \phi_r \right)\right)}, \quad (102)$$

$$\tan(\Theta_R) = \frac{C_N^1 r \sin(\delta + \sum_{k=1, k \neq 1}^N \phi_k) + C_N^2 r^2 \sin(2\delta + \sum_{r=1, r \neq 1, 2}^N \phi_r) + \dots + C_N^N r^N \sin(N\delta)}{C_N^1 r \cos(\delta + \sum_{k=1, k \neq 1}^N \phi_k) + C_N^2 r^2 \cos(2\delta + \sum_{r=1, r \neq 1, 2}^N \phi_r) + \dots + C_N^N r^N \cos(N\delta)}, \quad (103)$$

where  $C_N^k$  are the binomial coefficients,  $N \geq k \geq 0$ . Hence, the later expression can be bounded by

$$\left| Re^{i\Theta_R} \right| < \sqrt{\sum_{j=1}^N (C_j^N \varepsilon_{QSP}^j)^2 + 2 \sum_{j,k=1, j \neq k}^N C_k^N C_j^N \varepsilon_{QSP}^{j+k}} = \sum_{j=1}^N C_j^N \varepsilon_{QSP}^j = (1 + \varepsilon_{QSP})^N - 1 \sim N\varepsilon_{QSP}, \quad (104)$$

when  $N\varepsilon_{QSP} \ll 1$ . After renormalization we can write the state (101) as

$$|\Phi_N\rangle \sim \frac{|0\rangle + (e^{i\Phi_N} + Re^{i\Theta_R})|1\rangle}{\sqrt{2 + R^2 + 2R \cos(\Theta_R - \Phi_N)}} |\phi_1^N\rangle. \quad (105)$$

Applying the Hadamart gate, we get

$$H \otimes I |\Phi_N\rangle = \frac{(1 + e^{i\Phi_N} + Re^{i\Theta_R})|0\rangle + (1 - e^{i\Phi_N} - Re^{i\Theta_R})|1\rangle}{\sqrt{2}\sqrt{2 + R^2 + 2R \cos(\Theta_R - \Phi_N)}} |\phi_1^N\rangle. \quad (106)$$

Similarly to the procedure in previous sections, the probabilities to measure  $|0\rangle$  and  $|1\rangle$  are

$$P(X=0|\Phi_N) = \frac{1}{2} + \frac{R \cos(\Theta_R) + \cos(\Phi_N)}{2 + R^2 + 2R \cos(\Theta_R - \Phi_N)}, \quad P(X=1|\Phi_N) = \frac{1}{2} - \frac{R \cos(\Theta_R) + \cos(\Phi_N)}{2 + R^2 + 2R \cos(\Theta_R - \Phi_N)}. \quad (107)$$

If we act on the memory qubit with  $S$  gate and then do encoding, after all steps we get

$$|\Phi_N\rangle = \frac{|0\rangle + i(e^{i\Phi_N} + Re^{i\Theta_R})|1\rangle}{\sqrt{2 + R^2 + 2R \cos(\Theta_R - \Phi_N)}} |\phi_1^N\rangle. \quad (108)$$

Then we apply the Hadamart gate

$$H \otimes I |\Phi_N\rangle = \frac{(1 + i(e^{i\Phi_N} + Re^{i\Theta_R}))|0\rangle + (1 - i(e^{i\Phi_N} + Re^{i\Theta_R}))|1\rangle}{\sqrt{2 + R^2 + 2R \cos(\Theta_R - \Phi_N)}} |\phi_1^N\rangle \quad (109)$$

and the probability to measure  $|0\rangle$  and  $|1\rangle$  are

$$P(Y=0|\Phi_N) = \frac{1}{2} - \frac{R \sin(\Theta_R) + \sin(\Phi_N)}{2 + R^2 + 2R \cos(\Theta_R - \Phi_N)}, \quad P(Y=1|\Phi_N) = \frac{1}{2} + \frac{R \sin(\Theta_R) + \sin(\Phi_N)}{2 + R^2 + 2R \cos(\Theta_R - \Phi_N)}. \quad (110)$$

It is easy to check that the variable  $Q$  defined in (52) in this case is the following

$$Q = \frac{R \sin(\Theta_R) + \sin(\Phi_N)}{R \cos(\Theta_R) + \cos(\Phi_N)}. \quad (111)$$

To rewrite it, we use the arbitrary phase shifts *sine* rule:

$$a \sin(x + \theta_a) + b \sin(x + \theta_b) = c \sin(x + \varphi_{ab}), \quad (112)$$

where  $c$  and  $\varphi$  satisfy:

$$c^2 = a^2 + b^2 + 2ab \cos(\theta_a - \theta_b), \quad \tan \varphi_{ab} = \frac{a \sin \theta_a + b \sin \theta_b}{a \cos \theta_a + b \cos \theta_b}.$$

Then (111) can be rewritten as

$$Q = \tan \left( \Phi_N + \arctan \left( \frac{R \sin(\Theta_R - \Phi_N)}{R \cos(\Theta_R - \Phi_N) + 1} \right) \right) \sim \tan(\Phi_N + R \sin(\Theta_R - \Phi_N)) \sim \tan(\Phi_N + N\varepsilon_{QSP}). \quad (113)$$

Hence, the variance of the estimate of  $\Phi_N$  is

$$\begin{aligned} \sigma^2 \hat{\Phi}_N &\sim \frac{\cos^4(N\varepsilon + \Phi_N)}{4M_q(N\varepsilon \cos(\Theta_R) + \cos(\Phi_N))^4} (12N\varepsilon \cos(\Theta_R - \Phi_N) + 4N\varepsilon \cos(\Theta_R + 3\Phi_N) + \cos(4\Phi_N) + 3) \\ &\sim \frac{\cos(4\Phi_N) + 3}{4M_q} \sim \frac{1}{M_q}, \end{aligned} \quad (114)$$

where we used that  $|R| < N\varepsilon_{QSP}$ ,  $\varepsilon_{QSP} \ll 1$  and  $M_q$  is the amount of repetitions of reproduction of the encoded state.

Finally, we want to be sure that the standard deviation  $\sqrt{\eta}$  of the estimate  $\hat{O}$  is greater then the error inserted by the QSP approximation  $N\varepsilon_{QSP}$ . Hence we can conclude

$$\varepsilon_{QSP} \leq \frac{\sqrt{\eta}}{N}, \quad n_{QSP} = O \left( \frac{\log(\frac{N}{\sqrt{\eta}})}{\log \log(\frac{N}{\sqrt{\eta}})} \right). \quad (115)$$

### Phase Wrapping Estimation for QSP and Taylor Based Methods

The problem of phase wrapping also holds for the QSP based version of our method. We can use the strategy discussed above for the Taylor based method, where the series of projective measurements are used to control the amount of wrappings. However, this will significantly worsen the variance rate of the QSP based estimate.

One can see that a strategy of estimating the phase directly fail unless it is already known to sit within a window of width  $2\pi/k$ , where  $k$  is significantly large. To overcome this problem we can use method introduced in [30], and improved in [13] for the purpose of gate calibration. We select  $\tilde{\epsilon}_0 = 2\sqrt{\epsilon}$  and introduce the notation

$$(\phi_0)_{QSP} = \tilde{\epsilon}_0 P_{sum}, \quad P_{sum} \equiv \sum_{j=0}^N \tau_j |a_j \langle P_j \rangle|, \quad (116)$$

such that  $(\phi_0)_{QSP} < 2\pi$ , holds. Here we state the result:

**Algorithm .1.** *Given a targeted precision  $\eta > 0$ , and numbers  $\alpha, \gamma \in \mathbb{Z}^+$ , the algorithm outputting an estimate  $\hat{P}_{sum}$  as an estimate for  $P_{sum}$  proceeds as follows:*

- Fix  $d_L = \lceil \log_2 1/\eta \rceil$ .
- For  $l = 1, 2, 3, \dots, d_L$ :
  - Obtain an estimate  $(\hat{\phi}_l)_{QSP}$  for  $(\phi_l)_{QSP} = 2^l \tilde{\epsilon}_0 P_{sum} \bmod 2\pi$  from  $M_l = \alpha + \gamma(d_L + 1 - l)$  repetitions of Hadamard test circuit with  $K = I$  and  $K = S$ .
  - If  $l = 1$ , set  $\hat{P}_{sum}^{(1)} \equiv \frac{(\hat{\phi}_0)_{QSP}}{\tilde{\epsilon}_0}$ .
  - Else, set  $\hat{P}_{sum}^{(l)}$  to be the (unique) number in  $[\hat{P}_{sum}^{(l-1)} - \frac{\pi}{2^l}, \hat{P}_{sum}^{(l-1)} + \frac{\pi}{2^l})$  such that

$$2^l \tilde{\epsilon}_0 \hat{P}_{sum}^{(l)} \equiv (\hat{\phi}_{l-1})_{QSP}, \quad (117)$$

holds.

- Return  $\hat{P}_{sum} = \hat{P}_{sum}^{(d_L)}$  as an estimate for  $P_{sum}$ .

It was proved in [13] that, choosing  $\alpha > 2$  and  $\gamma > 0$ , the variance  $\eta$  on the final estimate scales like  $\sim cM^{-1}$ , where where  $c$  is a constant and  $M$  is a total cost.

Using (114), where  $M_q = 2 \sum_{l=0}^{d_L} M_l$ , the variance of the estimated observable by the QSP based method can be written as follows

$$\sigma^2(\hat{O}_{QSP}^{Qcor}) \sim \frac{1}{2^{2d_L} \tilde{\epsilon}_0^2 M_q}. \quad (118)$$

The total amount of state preparations for the QSP based method is  $T_{QSP} = N n_{QSP} M_q + M_1 = N(n_{QSP} M_q + n_1)$ , because for every Pauli string we do  $n_{QSP}$  QSP steps, we repeat it for  $N$  Pauli strings  $M_q$  times and  $M_1$  times we do projective measurements to estimate the sign of every Pauli string. The variance of the estimated observable scales as

$$\sigma^2(\hat{O}_{QSP}^{Qcor}) \sim \frac{n_{QSP}}{2^{2(d_L+1)} \epsilon (\frac{T_{QSP}}{N} - n_1)} \sim \frac{N}{T_{QSP}}, \quad (119)$$

where we selected  $\epsilon \sim 2^{-2(d_L+1)}$ . Then comparing the variances of the estimated observable by the QSP based method and by QEE one, we get

$$\frac{\sigma^2 \hat{O}_{QSP}^{Qcor}}{\sigma^2 \hat{O}_{QEE}} \sim \frac{1}{N}. \quad (120)$$

Note that we can use this algorithm for a Taylor based variation of our method. Then the amount of repetitions of the Hadamard test is  $M_q = 2 \sum_{l=0}^{d_L} M_l$  and the variance of the estimate is of the rate

$$\sigma^2(\hat{O}_T^{Qcor}) \sim \frac{1}{2^{2(d_L+1)} \epsilon M_q} + \frac{\epsilon^2 N^2}{M_c^{cor}}. \quad (121)$$



The optimal  $\epsilon$  selection that minimizes the variance is

$$\epsilon = \left( \frac{M_c^{cor}}{2^{2(d_l+1)} M_q} \right)^{\frac{1}{3}} \frac{1}{N^{\frac{2}{3}}}. \quad (122)$$

Then the variance (121) can be written as follows

$$\sigma^2(\hat{O}_T^{Qcor}) \sim \frac{N^{\frac{2}{3}}}{M_q^{\frac{2}{3}} (M_c^{cor})^{\frac{1}{3}} 2^{\frac{4}{3}d_L}}. \quad (123)$$

The total amount of the state preparations used in the Taylor based method is  $T_T = (1 + n_{QPE})NM_q + M_c^{cor}$  and then the final expression is the following

$$\sigma^2(\hat{O}_T^{Qcor}) \sim \frac{N^{\frac{4}{3}} n_3^{\frac{2}{3}}}{T_T 2^{\frac{4}{3}d_L}}, \quad (124)$$

where we still get  $1/N^{\frac{2}{3}}$  overhead in variance comparable to QEE method, eliminating the condition (84).

### CPS Algorithm

Our method contains five stages illustrated in Fig. 4.

- In *stage 1*, we perform projective measurements  $M_c^{cor}$  ( $M_1$ ) times to estimate  $\langle P_j \rangle$ ,  $j = 1, \dots, N$ . In the Taylor based method (1) we are using the elements of the QPE circuit in the encoding part of the method. Thus we must be sure that  $|\langle P_j \rangle|$  is bounded away from 0 and 1 to guarantee its performance.
- We classically verify this bounds in *stage 2*. If  $|\langle P_j \rangle|$  is not bounded, we continue with statistical sampling, doing more projective measurements, to estimate the expectation with the final required uncertainty. The information about  $|\langle P_j \rangle|$  is stored classically. In the QSP based method (2) we need this information to estimate  $\tau_j = \text{sign}(|a_j \langle P_j \rangle|)$ .
- Next three stages we repeated for every  $\tilde{\epsilon}_l$  parameter  $M_l$ ,  $l = 1, \dots, d_L$  times. The encoding *stage 3* contains two steps. For method (1) in the *stage 3.1.j.*, if  $|\langle P_j \rangle|$  is bounded away from 0 and 1 we use the QPE circuit to resolve between  $|\phi^+\rangle$  and  $|\phi^-\rangle$ . We construct the state  $|\tilde{\Psi}_0\rangle_j^{\tilde{\epsilon}_l}$  and initialize the ancillary qubits  $|a_{temp}\rangle$ . Subsequently, we proceed  $n_{QPE}$  rounds of QPE based on  $U_{P_j}$  for every Pauli string. In *stage 3.2.j.*, we apply the controlled unitary rotation  $\tilde{U}_{P_j}$  and  $\tilde{U}_{P_j}^\dagger$  to  $|\phi^+\rangle$  and  $|\phi^-\rangle$ , respectively, to encode the phase  $\phi_j$  with the correct sign into the memory qubit  $|a_m\rangle$ . This stage is repeated as many times as the number of Pauli strings that are bounded away from 0 and 1 (maximum  $N$  times). The total amount of QPE applications is maximum  $M_{QPE} = Nn_{QPE}$  for all the Pauli strings in one round of encoding. In method (2) we do not need the QPE step. Instead we proceed an  $n$ -degree optimal trigonometric polynomial approximations of  $e^{i\tau_j \phi_j^{\tilde{\epsilon}_l}}$  for every Pauli string. We use the measurements from *stage 1* for  $\tau_j$  estimation. Doing the QSP approximation sequentially for all  $N$  Pauli strings we encode all the sum in the memory qubit.
- In *stage 4* for both methods (1) and (2), we perform a projective measurement to estimate  $\Phi_N^{\tilde{\epsilon}_l}$ . For (1), we use Eq. (18) to extract the knowledge about  $\sum_{i=1}^N |a_i \langle P_i \rangle|$ .
- Finally, for (1) in *stage 5*, we use the measurements from *stage 1* for correction.

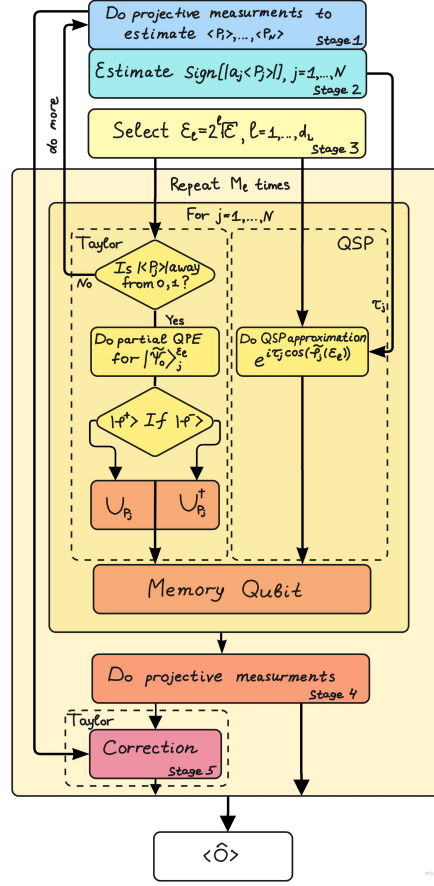


FIG. 4. The outline of the proposed method. In the *stage 1-2* we roughly estimate the  $\langle P_j \rangle$  by a series of projective measurements. Using this knowledge, stored classically, in *stage 3* (1) we prepare  $|\Psi_0\rangle$  and perform a partial projection to encode each Pauli string with the correct sign in the long coherent time qubit  $|a_m\rangle$ . In (2) we do QSP to encode every Pauli string in the memory qubit getting rid of  $\arccos(\cdot)$  function. Next, we perform a final projective measurement on the state encoded in  $|a_m\rangle$ . The *stage 3* is repeated many times to obtain statistics for the estimate of the mean value of the observable. Finally, for (1) in *stage 5* we perform the error correction, using *stage 1* results.

$$|\phi^+\rangle$$